



Corrigendum to “What happens to fracture energy in brittle fracture? Revisiting the Griffith assumption” published in Solid Earth, 10, 1385–1395, 2019

Timothy R. H. Davies¹, Maurice J. McSaveney², and Natalya V. Reznichenko¹

¹Department of Geological Sciences, University of Canterbury, Christchurch 8140, New Zealand

²GNS Science Ltd, P.O. Box 30368 Lower Hutt 5040, New Zealand

Correspondence: Timothy R. H. Davies (tim.davies@canterbury.ac.nz)

Published: 11 August 2021

During the submission of the paper an error occurred in the calculation of the factor k in Table 2. Below is the corrected Table 2, with corrected values in bold.

Table 2. The k values derived from fragment SEM images.

Number of fragments in image	P_{2df}/P_{2dec} max	k maximum	k average
144	2.378	2.38	3.9
285	2.925	2.93	4.1
105	2.628	2.63	4.1

The paragraph following Eq. (5) is correspondingly amended as follows.

The average k values in Table 2 are close to 1.4. These will be underestimates because our calculation assumes that there is no irregularity of the fragments in the dimension not shown in the images, suggesting increasing the k values by 33%. Thus, in estimating fragment surface areas we have used $k = 1.7$. This is much lower than values (generally 5–10; Chester et al., 2005; Hochella and Banfield, 1995; White et al., 1996) found for rock fragments.

Table 3 is also affected by this change. Below is the corrected Table 3, with corrected values in bold.

Table 3. Pyrex fragmentation data from Kolzenburg et al. (2013) (Kolz.) and from the present study (UC).

Sample name	Confining pressure MPa	Peak stress MPa	Stress drop MPa	Post-failure strength MPa	Total energy J	Surface area m ²	Theoretical surface area m ² ($U = 4.28$)
Kolz. 1	25	1277	1251	26	148.5	127.52	34.70
Kolz. 2	50	1046	842	204	145.7	88.16	34.04
Kolz. 3	75	1051	756	295	161.3	59.32	37.69
Kolz. 4	100	1293	761	532	179.9	54.88	42.03
Kolz. 6	15	1389	1372	18	146.3	184.22	34.18
Kolz. 7	5	835	825	10	75.5	97.66	17.64
Kolz. 8	0.1	648	645	3	52.3	67.9	12.22
UC1	0	917	917	0	133.2	30.6	31.12
UC2	0	606	606	0	46.6	7.5	10.89
UC3	0	500	500	0	38.9	4.1	9.09
UC4	0	667	667	0	43.7	4.7	10.21

As a result of these changes, Fig. 8 is also amended. Below is the corrected Fig. 8.

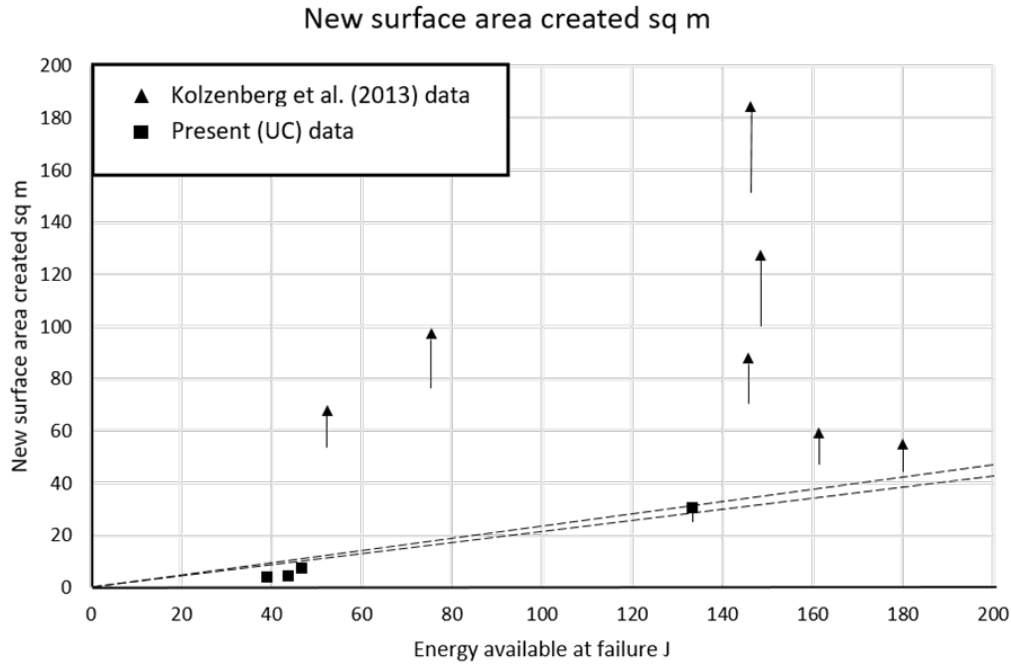


Figure 8. Experimental data from the present work (squares) and from Kolzenburg et al. (2013) (triangles) showing the new surface created by failures involving various energies. The dashed lines show the upper limit on surface area imposed by the specific surface energy of Pyrex ($4.5 \pm 0.22 \text{ J m}^{-2}$) if the energy used for fracture is lost to surface energy. Vertical lines descending from data points indicate extreme possible negative errors. It is notable that most of the data points lie above this, and some are considerably above. The maximum theoretical strain energy that can be stored in Pyrex is $Q^2/2E \text{ J m}^{-3}$ (Herget, 1988; Q is the unconfined compressive strength of the material and E is its elasticity); this is about 200 J in the experimental cylinders.

These revisions, in particular the revised Fig. 8, require amendments to the commentary on the outcomes of the work. We have reworded our Sect. 4 as follows.

Acknowledgements. We are grateful to Won Joon Song and Scott Johnson at the University of Maine, USA, for identifying and drawing our attention to the error in our original calculations.

4 Data

The experimental data from our tests and those of Kolzenburg et al. (2013) are listed in Table 3 and illustrated in Fig. 8. Table 3 and Fig. 8 show that in most cases more new surface area was created than would be possible if the Griffith (1921) assumption were valid (i.e. all the elastic strain energy used to create new surface area – FSE – became surface free energy – SFE). The maximum possible accumulated errors arising from neglect of machine energy are shown as vertical lines descending from the data points in Fig. 8. Thus, the possible inaccuracies in our data do not affect the overall result.

Similarly, the effect of possible variations in the specific fracture energy of borosilicate glass ($4.5 \pm 0.22 \text{ J m}^{-2}$; Wiederhorn, 1969) is included in the location of the dashed lines in Fig. 8 and has a negligible effect. The theoretical maximum surface area corresponding to the energy available is also estimated (Table 1, final column), assuming that the specific fracture energy is 4.28 J m^{-2} . The data in Table 3 and Fig. 8 indicate that up to 5 times more surface area was created than allowed by the Griffith assumption; this strongly suggests that the assumption is not valid.

Our (UC) data were obtained in air at ambient humidity, whereas the data of Kolzenburg et al. (2013) were obtained in a dry (argon) atmosphere. It is known that the presence of water vapour reduces the specific fracture energy of Pyrex (Wiederhorn, 1969), and this could affect our data; however, it is difficult to envisage how moisture in the outside atmosphere could affect the interior of an impermeable (non-crystalline) cylinder. Thus, the new surface would have been generated under moisture-free conditions in our experiments, to which the specific surface energy of 4.5 J m^{-2} applies. Nevertheless, the distinct difference in the UC and Kolzenburg et al. (2013) data may be due to this factor.

We assume that ultrasonic treatment only disaggregates particles that are weakly bonded to each other and is not able to fracture intact glass. In order to test this assumption we subjected $500 \mu\text{m}$ glass beads to ultrasound at the same intensity and for the same duration as the Pyrex fragments; we found no difference in size distribution between pre- and post-ultrasound analysis, and SEM examination confirmed the lack of breakage of the glass beads. Since the ultrasonic energy density required to break particles is inversely related to their size (Knoop et al., 2016), we concluded that ultrasound treatment did not cause the breakage of intact micron-scale Pyrex fragments, only disaggregation of previously agglomerated or previously cracked grains.